Sensing and Bio-Sensing Research 21 (2018) 27–34

Contents lists available at ScienceDirect

Sensing and Bio-Sensing Research

journal homepage: www.elsevier.com/locate/sbsr

Electrochemical determination of phenothrin in fruit juices at graphene oxide-polypyrrole modified glassy carbon electrode

Molla Tefera[a], Merid Tessema[b], Shimelis Admassie[b], Emmanuel I. Iwuoha[c], Tesfaye T. Waryo[c], Priscilla G.L. Baker[c,*]

[a] Department of Chemistry, University of Gondar, P. O. Box 196, Gondar, Ethiopia
[b] Department of Chemistry, Addis Ababa University, P. O. Box 1176, Addis Ababa, Ethiopia
[c] Sensor Lab, Department of Chemistry, University of the Western Cape, Private Bag X17, Robert Sobukwe Drive, Bellville 7535, South Africa

ARTICLE INFO

Keywords:
Phenothrin
Graphene oxide-polypyrrole
Sensor
Fruit juices

ABSTRACT

An electrochemical sensor was developed based on graphen oxide-polypyrrole modified glassy carbon electrode (GO/PPy/GCE) for sensitive determination of phenothrin in fruit samples. GO/PPy/GCE was characterized by scanning electron microscopy (SEM), Fourier Transform Infrared Spectroscopy (FT-IR), Ultraviolet-Visible spectroscopy (UV–Vis) and Raman spectroscopy. The sensor was also characterized using electrochemical impedance spectroscopy and cyclic voltammetry. Compared to bare GCE, GO/GCE and PPy/GCE, the reduction peak current of phenothrin increased significantly at GO/PPy/GCE, demonstrating that GO/PPy/GCE exhibited electrocatalytic activity towards the reduction of phenothrin. Under the optimal conditions, the sensor showed a linear relationship over the range of 2.5×10^{-8}-2.0×10^{-5} M with detection limits of 13.8×10^{-9} M. In addition, the analytical application of the proposed method was carried out by the determination of phenothrin in fruit juice samples.

1. Introduction

Pyrethroids are synthetic insecticides with structures based on the natural chemicals pyrethrins. They are broad spectrum, low resistant to pests and low mammalian toxicity, highly stable to light and temperature and are very lipophilic compounds. Due to these properties, they are widely used in pest control in agriculture, public health, horticulture and veterinary applications [1–8].

Phenothrin ($C_{23}H_{26}O_3$) belongs to type I pyrethroids with chrysanthemate moiety non-cyanopyrethroid insecticide. It has been used extensively to control pests in agricultural crops such as vegetables, fruits, potatoes, cereals and household insects. Although phenothrin is thought to be low toxicity to humans, the residues left after its use can cause endocrine-disrupting diseases and depolarization to humans and paralyze the peripheral and central nervous system [9]. Its general routes are through inhalation of household aerosol sprays, ingestion of food containing residual material, or dermal contact with pediculicides.

Owing to its toxicity, it is necessary to develop a rapid and an effective method for the determination of phenothrin in food samples. Analytical techniques such as gas chromatography [8,10], gas chromatography with mass spectrometry [11], electrophoresis [12] and immunoassay methods [13] have been most widely used for the determination of phenothrin. Despite of their advantageous, most of these techniques require relatively expensive instrumentation, long times of analysis, and trained personnel [14–16]. However, due to low cost, minimum or no sample pretreatment, simplicity, fast response, good sensitivity and high selectivity, electrochemical techniques are alternative methods for the determination of phenothrin. Thriveni et al. [17] reported an electrochemical sensor based on a hanging mercury drop electrode for the determination of phenothrin in agricultural formulations, vegetables, and storage bags of wheat and rice samples.

Graphene oxide (GO) is an oxidation by-product of graphite with its base made of oxygen-containing groups. Recently, GO has received a great interest due to its low cost, easy access, and widespread ability to be converted in to graphene. Depending on the amount of oxidant and oxidation time, GO contains multiple defects. The ability for graphene oxide to conduct electrons depends on the amount of oxidizing agent as well as the method of synthesis [18]. Furthermore, oxygen-containing groups also enable GO to exhibit excellent hydrophilic properties which further allows its interaction with nanomaterials and polymers to form composites [19,20]. High surface-to-volume ratio of GO, in conjunction with its high dispersibility in both water and organic solvents as well as its wide range of reactive surface-bound functional groups, GO-based materials have been used to devise and prepare GO-based electrodes for

* Corresponding author.
E-mail address: pbaker@uwc.ac.za (P.G.L. Baker).

https://doi.org/10.1016/j.sbsr.2018.09.003
Received 18 March 2018; Received in revised form 13 September 2018; Accepted 24 September 2018

a wide range of applications in electrochemical sensors and electroanalysis [21,22]. Based on the properties of GO mentioned above, considerable attention has been devoted in exploring hybrid of different materials for various applications.

Polypyrrole is also a promising material for electrochemical sensors and energy storage devices owing to its good electrical conductivity, high energy storage capacity and electrochemical reversibility [21,23,24]. Recently, composites of GO-PPy have also become appealing sensor materials because of their combined effects, and better electrochemical performance than each component [25]. The composites of GO-PPy have been fabricated as a promising material for supercapacitors [26–28], solar cell [29] and glucose biosensor [30]. Thus, in this study, we report the use of graphene oxide-polypyrrole composite modified glassy carbon electrode for the determination of phenothrin in various fruit juices.

2. Experimental

2.1. Chemicals

Graphite (Aldrich, 282,863), pyrrole (Sigma Aldrich, 131,709, 98%), phenothrin (Sigma Aldrich, 36,193, 94.4%), phoxim (Sigma Aldrich, 36,197, 98%) and ascorbic acid (Sigma Aldrich, A7506, RG), dichlorvos (Sigma Aldrich, 45,441, 98.8%), urea (Fluka, 2493, 99.5%), $NaNO_3$ (Sigma Aldrich, S5506, 99%), $KMnO_4$ (Sigma Aldrich, 399,124, 99%), H_2O_2 (Sigma Aldrich, 30%wt in H_2O, 216,763), $LiClO_4$ (Aldrich, 431,567, 99.99%), citric acid (Sigma Aldrich C0759), KH_2PO_4 (Sigma Aldrich, 0662, 99%) and K_2HPO_4 (Sigma Aldrich, 3786, 98%). Standard solution of phenothrin was prepared in ethanol. Phosphate buffer solution (PBS) was obtained by mixing K_2HPO_4 and KH_2PO_4.

2.2. Instruments

All voltammetric measurements were carried out using PalmSens Trace (Palm Instruments BV, Utrecht, Netherlands) connected to a personal computer. A three electrode system in which GCE (3.0 mm diameter, Sigma Aldrich), GO/GCE, PPy/GCE and GO/PPy/GCE were employed as working electrodes, silver-silver chloride electrode (3 M NaCl) and platinum wire (1.0 mm diameter) were used as reference and counter electrode, respectively. Electrochemical impedance spectroscopic measurements (EIS) were performed on a CHI604D electrochemical workstation (CH Instruments, Inc., Austin, Texas, USA).

UV–Vis spectra were recorded on a Nicolette Evolution 100 Spectrometer (Thermo-Electron Corporation, UK). FTIR spectra were recorded on a Perkin Elmer Spectrum 100-FTIR spectrometer (Waltham, USA). Raman Horiba Scientific Xplora, Olympus BX41 Raman Spectrometer (France) was used for the Raman spectroscopic analysis.

Morphology and compositions of GO, PPy and GO/PPy composite were examined using scanning electron microscopy (AURIGA, Field Emission Gun High resolution Scanning Electron Microscope (FEG HRSEM, Zeiss)) and Raman spectra were measured by Triax 320 Raman system (Jobin-Yvon, Inc., Longjumeau, France), equipped with 632.8 nm He/Ne laser line as excitation source (JDS Uniphase Corporation, Milpitas, CA) and liquid-nitrogen cooled Ge array detector (Jobin-Yvon, Inc.). Screen printed carbon electrodes were used for the electrodeposition of PPy, GO and GO/PPy composite for SEM measurements.

2.3. Synthesis of graphene oxide

GO was synthesized from graphite using the modified Hummer's method following a procedure similar to that reported by Hanifah et al. [31]. 3.0 g of $NaNO_3$ was dissolved in 140 mL of conc. H_2SO_4 in an ice bath. Next, 15 g of $KMnO_4$ and 3 g of graphite powder were added gradually into the above mixture. The temperature was maintained below 20 °C with vigorous stirring using a mechanical stirrer. The temperature of this mixture was then increased and maintained to 35 °C. The mixture was continuously stirred for 12 h at this temperature and the resulting solution was diluted with double distilled water under vigorous stirring. Consequently, 20 mL of H_2O_2 and 800 mL of double distilled water were added into the mixture. The color of the mixture was observed changing from brown to brilliant yellow. Then, the mixture was washed with HCl and water followed by repeated centrifugation and filtration until the pH of filtrate became neutral. Lastly, the final product was washed and dried in vacuum.

2.4. Synthesis of GO/PPy/GCE

20 mg GO was dispersed in 10 mL of double distilled water (2 mg mL^{-1}) followed by ultrasonication for 30 min. The electrolyte was purged before voltammetric experiments for 10 min with highly purified N_2 in order to eliminate the adsorbed oxygen. GO/GCE was prepared by drop coating GO solution on GCE. Whereas, GO/PPy/GCE composite was prepared by electrochemical polymerization of a mixture containing 30 μL of GO suspension and 10 μL of 0.25 M pyrrole in 0.1 M $LiClO_4$ using cyclic voltammetry by scanning the potential from −1.2 to 0.6 V at a scan rate of 0.05 V s^{-1} for 8 cycles.

2.5. Sample preparation

Apple, grape and orange juices were purchased from Pick and Pay supermarket (Krush 100% Juice Blend) at Bellville suburb of Cape Town, South Africa. After centrifuging and filtering each juice sample, 5 mL clear solution of each juice sample was diluted with 10 mL of PBS pH 6.5. The samples were spiked with stock solution of phenothrin in PBS for recovery test.

3. Results and discussion

3.1. Characterization of GO/PPy composite

In order to ensure that the GO/PPy composite was successfully produced, the surface morphology of the electrode was characterized using microscopic and spectroscopic methods. The surface morphology of the GO and GO/PPy composite was characterized using SEM. As shown in Fig. 1A, GO shows a rough surface with many wrinkles, showing a three-dimensional morphological microstructure due to the presence of GO sheets. On careful looking a slight change in the morphology of GO/PPy can be observed, which confirms the formation of GO/PPy composite (Fig. 1B).

FTIR spectra of GO, PPy and PPy/GO are shown in Fig. 2. For the GO sample, the broad peak at 3431 cm^{-1} corresponds to O—H stretching, which is responsible for good dispersibility in water [31]. The peaks at 2924 and 2848 cm^{-1} are assigned to symmetric vibration and asymmetric stretching peaks of aromatic CH_2 group [30,32,33]. Peaks at 1640 cm^{-1} and 1740 cm^{-1} can be attributed to the aromatic C=C stretching vibration and the carbonyl (C = O) stretching, respectively [31]. The absorption peaks at 1539 cm^{-1} corresponds to the C=C stretching of the aromatic ring of GO [30]. Finally, the absorption peaks 1295 cm^{-1}, 1163 cm^{-1} and 1073 cm^{-1} correspond to C-OH of carbonyl, C-OH of alcohol and C—O of epoxy group, respectively [33].

For PPy, the absorption peaks at 3180 cm^{-1}, 1650 cm^{-1} and 1405 cm^{-1} correspond to N—H, C—N and C—C stretching vibration in the polypyrrole ring, respectively. In addition, the band at 1108 cm^{-1} is attributed to the C—H in plane vibration of pyrrole ring [32–34].

In the composite GO/PPy, the characteristic peaks of PPy at 1650 cm^{-1} and 1405 cm^{-1} have been shifted to 1454 cm^{-1} and 1717 cm^{-1}, respectively. This is most likely caused by π–π interaction between the GO layers and aromatic polypyrrole rings. Furthermore, a broad peak with decreased in size exhibited at 3431 cm^{-1}, which are attributed to the hydrogen bonding between the GO layers and

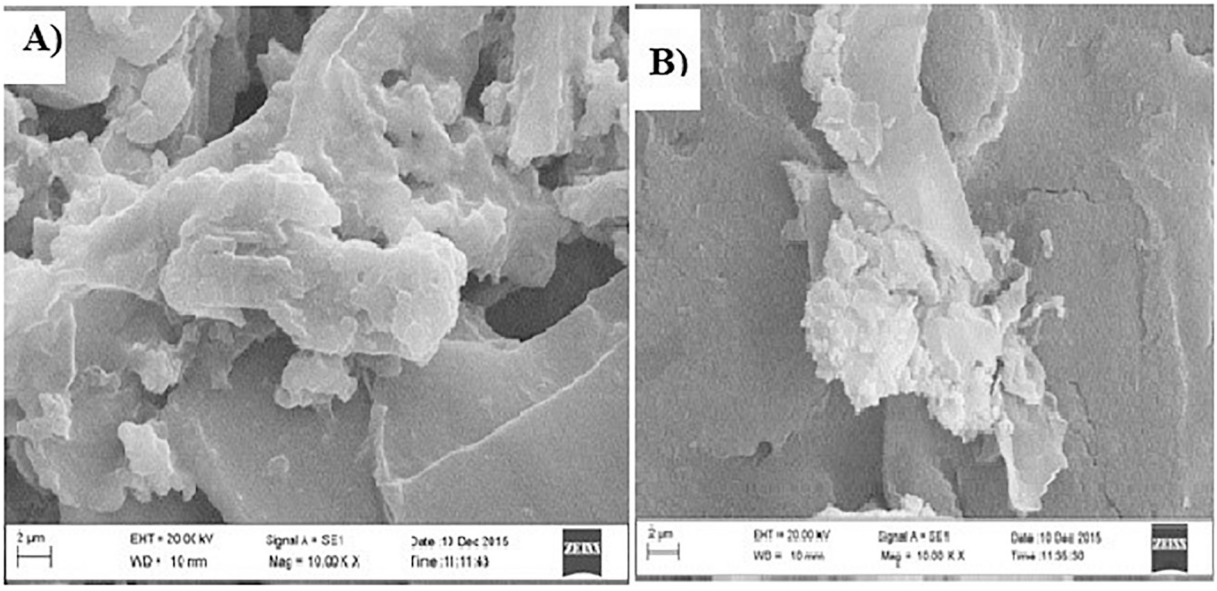

Fig. 1. SEM images of the GO (A) and GO/PPy (B).

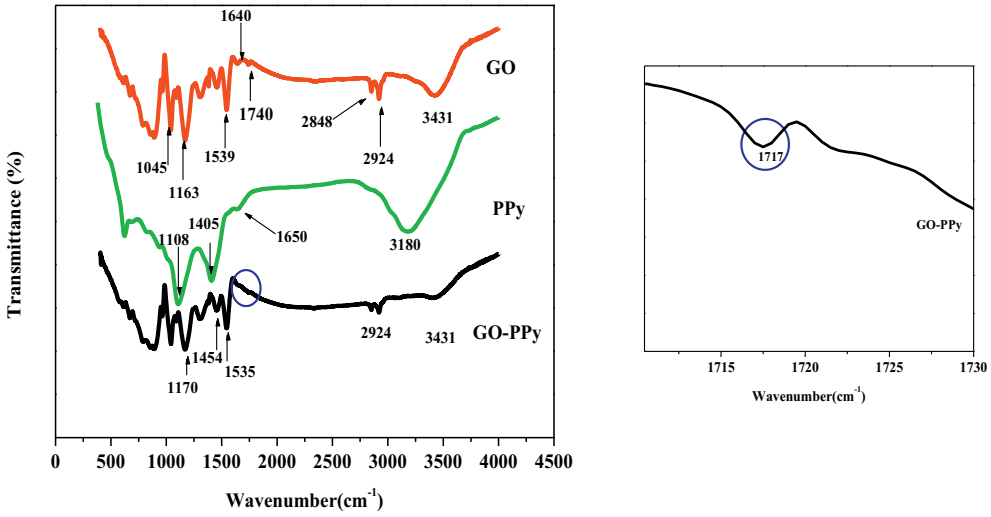

Fig. 2. FTIR spectra of GO, PPy and GO/PPy.

aromatic polypyrrole rings. The peak due to C═O of GO shifted towards lower wave number, which indicates that the electron density around the surface groups on the GO dispersed in polypyrrole polymer in forming the composite. However, the other characteristic peaks of GO were found in the spectrum of PPy/GO composite with decreased in intensity. These results suggest that GO has been successfully incorporated into the PPy film [35,36].

Fig. 3 shows the UV–Vis spectra of GO and GO/PPy. The spectrum of GO shows absorption band at 322 nm and 457 nm, corresponding to the π-π* transition of the conjugated aromatic double bonds (C = C) and n-π* transitions of the carbonyl groups, respectively [37]. After the polypyrrole electropolymerized in the presence of GO (GO/PPy), absorption peaks were observed at 260 nm and 322 nm, which are attributed to π-π* transitions and n-π* transitions, respectively. A shoulder-like appearance observed over the range 400 nm to 520 nm corresponds to the polaronic and bipolaronic transition (n-π* transition) which are the feature of the oxidized state of PPy segments. The change in the intensity of the absorption band and appearance of new band in GO/PPy indicates the electronic structure of GO was changed

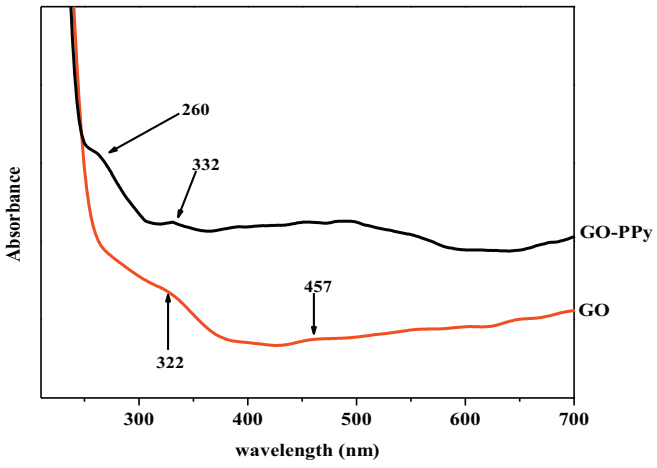

Fig. 3. UV–Vis spectra of GO, PPy and GO/PPy.

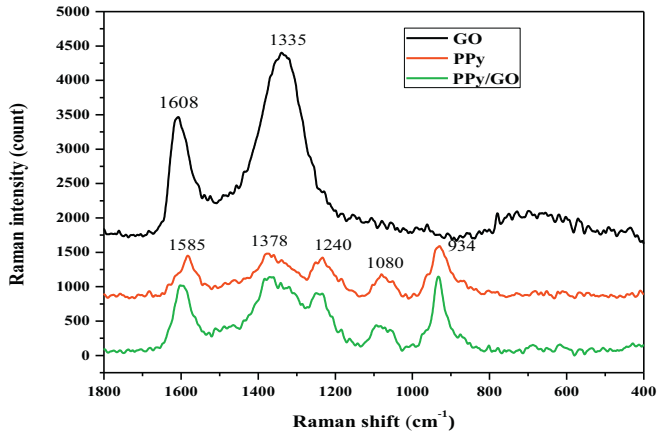

Fig. 4. Raman spectra of GO, PPy and GO/PPy.

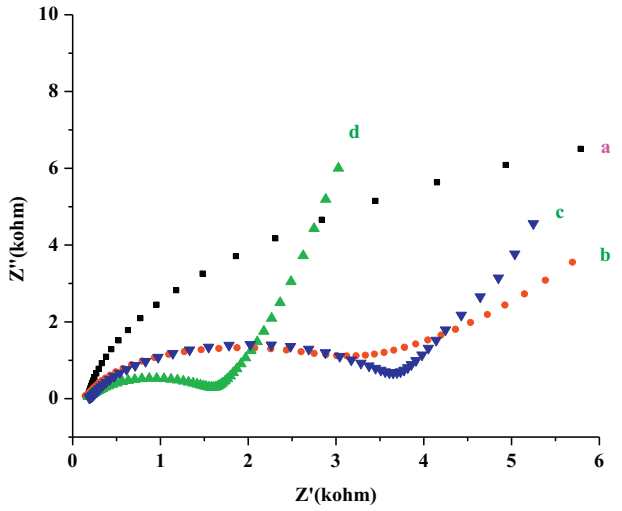

Fig. 5. Nyquist plots of 0.1 mM phenothrin at bare GCE (a), PPy/GCE (b), GO/GCE (c) and GO/PPy/ GCE (d).

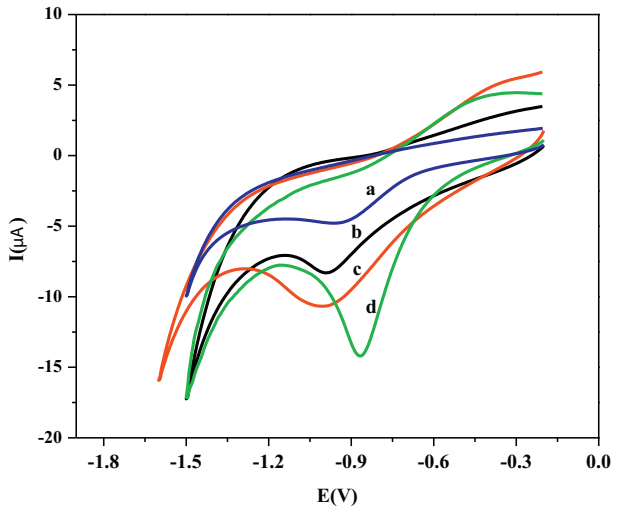

Fig. 6. Cyclic voltammograms of 10 μM phenothrin in PBS (pH 7.0) at GCE (a), GO/GCE (b), PPy/GCE (c) and GO/PPy/GCE (d) at 0.1 V s^{-1}.

due to its interaction with PPy as a result of polymerization of pyrrole monomers. The energy of π-π* transitions of aromatic C=C bonds in GO has changed significantly by the addition of PPy, which is very likely caused by the π-π stacking between PPy and GO [37–40]. The UV–Vis results provide a good agreement with the FTIR results.

The Raman spectrum of GO (Fig. 4) shows two characteristic bands at 1335 cm^{-1} (D band) and 1608 cm^{-1} (G band). The D band corresponds to the structural imperfections created by the attachment of oxygenated groups on the carbon basal plane, while the G band is related to the in-plane vibration of sp^2 carbon atoms in a 2D hexagonal lattice. The intensity ratio of the D- and G-bands (I_D/I_G) indicates the degree oxidation and the size of sp^2 ring clusters in a network of sp^3 and sp^2 bonded carbon.

In PPy, the band that appeared at 1585 cm^{-1} is attributed to the C=C backbone stretching of PPy and the band at 1373 cm^{-1} could be due to the ring-stretching mode of PPy. In addition, the bands in the range of 1080 cm^{-1} to 1240 cm^{-1} which are associated to the C–H in-plane deformation of the PPy and the band at 934 cm^{-1} is assigned to the ring deformation associated with dication (bipolaron) and radical cation (polaron) formation.

As shown in the Raman spectrum of GO/PPy composite, there are two bands at 1595 cm^{-1} and 1375 cm^{-1} with decrease in intensity compared with the bands for GO, confirming decrease in the disorder due to the increase in size of the in-plane sp^2 domains in the presence of PPy. Furthermore, the intensity ratio of the D and G bands (I_D/I_G) decreased from 1.27 (GO) to 1.08 (GO/PPy), indicating a decrease in the defect sites [27,41–45].

3.2. Electrochemical behaviors of phenothrin

To demonstrate the successful development of GO/PPy/GCE sensor, electrochemical impedance spectroscopy was used to get information on the impedance changes of the sensor interface in the modification process. Electrochemical impedance spectra of phenothrin were analyzed in the frequency range of 1 Hz and 1 × 10^5 Hz at GCE, GO/GCE, PPy/GCE and GO/PPy/GCE. From the Nyquist plots (Fig. 5), R_{ct} values for different electrodes were found to increase in the order: GO/PPy/GCE < PPy/GCE < GO/GCE < GCE. GO/PPy/GCE shows the smallest semicircle at mid-high frequency regions because of its large surface area, high electrical conductivity, which can be accounted by the interaction of oxygen containing functional groups in GO and polypyrrole through π-π interaction and H-bonding well improving the contact rate of the composite and electrolyte.

The redox behavior of phenothrin studied using cyclic voltammetry. Fig. 6 shows typical cyclic voltammograms at GCE (a), GO/GCE (b), PPy/GCE (c) and GO/PPy/GCE (d) for 10 μM phenothrin in phosphate buffer solutions (pH 7.0) at a scan rate of 0.1 V s^{-1}. In all the voltammograms, only a reduction peak was observed without oxidation peak in the reverse direction as reported in previous works [17]. The reduction peak of phenothrin at the surface of glassy carbon is weak and broad due to slow transfer of electrons. However, at the modified electrodes the peak current responses are significantly enhanced. Moreover, at GO/PPy/GCE a remarkably sharp peak was observed at about −0.89 V, which showed 1.5-fold increase in cathodic current response compared to that at PPy/GCE (curve c), 1.7 fold to that at GO/GCE (curve b) and 3.2-fold at GCE (curve a). The results suggest that the GO/PPy film possess a more pronounced effect on the reduction of phenothrin than at GO or PPy. This can be attributed to the synergistic effect of fast electron transfer rate, large surface area; high electrical conductivity and increased active sites leading to high catalytic activity of GO/PPy/GCE. Furthermore, the adsorption of phenothrine is more feasible for due to π-π interactions of graphene oxide, polypyrrole and phenothrin which contribute to peak current enhancement.

3.3. Effects of scan rate and pH

In order to obtain the optimum experimental conditions, parameters such as pH and scan rate that can affect the peak current and peak

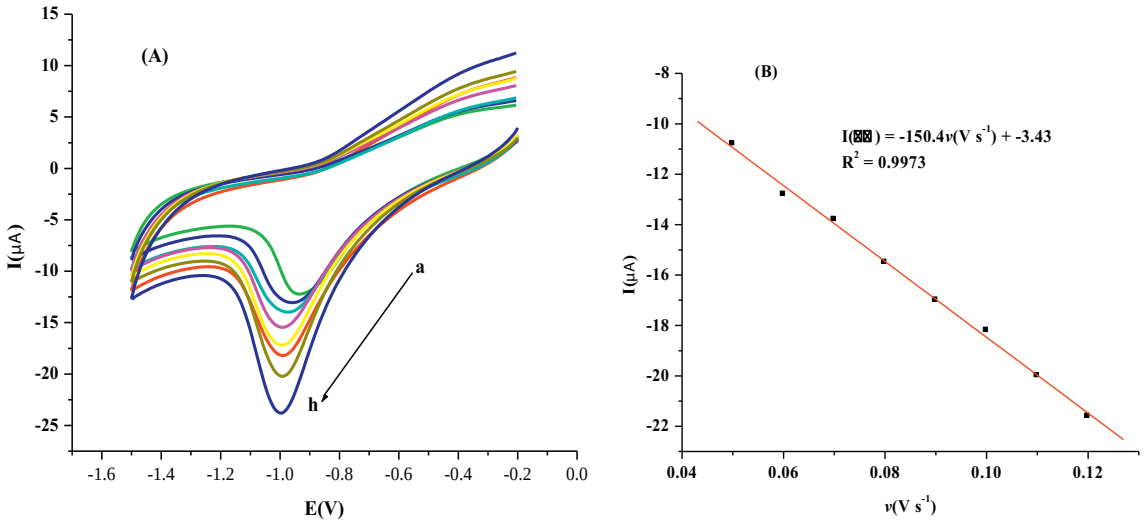

Fig. 7. Cyclic voltammograms of 10 μM phenothrin in phosphate buffer solution of pH 7.0 at GO/PPy/GCE for various scan rates: (a) 0.05, (b) 0.06, (c) 0.07, (d) 0.08, (e) 0.09, (f) 0.1, (g) 0.11 and (h) 0.12 V s^{-1} (A) and plot of current *vs* scan rate (B).

potential were studied for phenothrin solution at GO/PPy/GCE. The effect of the scan rate on the current response of phenothrin in phosphate buffer solution of pH 7.0 was studied using cyclic voltammetry (Fig. 7A). With increased scan rate, the cathodic peak current also increased. A good linearity was observed between the peak current and scan rate in the range 0.05–0.12 V s^{-1} (Fig. 7B), which shows that the reduction of phenothrin at GO/PPy/GCE is an adsorption process. Their linear relationship is described with the regression equation:

$$I(\mu A) = -150.4v + -3.43,\ R^2 = 0.9973 \quad (1)$$

Furthermore, with increase in the scan rate, the potential shifted to more negative values, which confirms the irreversible electrochemical behavior of phenothrin reduction at GO/PPy/GCE. The linear relationship between the peak potential and the logarithm of the scan rate can be expressed using the regression equation:

$$E_{pc}(V) = -0.13 \log v + -1.12,\ R^2 = 0.9960 \quad (2)$$

According to Laviron theory [46], the E_{Pc} and v can be related by the following equation for a totally irreversible process:

$$E = E^o + 2.303\left(\frac{RT}{\alpha nF}\right)\log\left(\frac{RTk^0}{\alpha nF}\right) - 2.303\left(\frac{RT}{\alpha nF}\right)\log v \quad (3)$$

where α is the transfer coefficient, k^o is the standard heterogeneous rate constant of the reaction, n is the number of electrons transferred, v the scan rate and E^o is the formal redox potential. Other symbols have their usual meanings. After substituting the values of T, R and F in Eq. (3), the value of αn was calculated to be 0.445. To determine the number of electrons transferred (n), the value of α is calculated using the equation:

$$\alpha = \frac{47.7}{E_p - E_{p/2}}mV \quad (4)$$

From this, the value of α was found to be 0.23. Thus, the number of electrons transferred in the electro-reduction of phenothrin was calculated to be 1.94 ≈ 2, that indicates two electrons are involved in the reduction of phenothrin as shown in the mechanism (Scheme 1) [17].

The effect of pH on the electrochemical behavior of phenothrin was studied in the range 5.0 to 8.0 in phosphate buffer solutions. It was found that the peak current increased with increasing of pH values from 5.0 to 6.5 and then decreased when the pH exceeded 6.5 (Fig. 8). Thus, pH 6.5 was selected as an appropriate working pH for phenothrin determination.

In addition, with increase in pH, the reduction peak potential shifted towards more negative values. The shift in the values of reduction potential indicates the participation of protons in the electrode reaction. A plot of peak potential *vs* pH values was found to be linear over the pH range of 5.0–8.0 with a regression equation of:

$$E(V) = -0.061pH + -0.41,\ R^2 = 0.9950 \quad (5)$$

The slope − 0.061 V/pH, which is close to the theoretical value of − 0.059 V/pH, indicates that the same number of protons and electrons are involved in the reduction of phenothrin [17].

3.4. Effects of accumulation potential and time

The sensitivity of the sensor is undoubtedly improved by varying accumulation parameters: potential and time. The effect of varying the accumulation potential on the reduction current of phenothrin was studied in the range − 0.3 to − 1.0 V at an accumulation time of 25 s. The current response increased up to − 0.7 V and decreased after − 0.7 V (Fig. S1A). Therefore, the accumulation potential of − 0.7 V was chosen as an optimum potential for further measurements.

The effect of accumulation time on the reduction peak current for 10 μM phenothrin was also investigated by SWV, and the results are illustrated in Fig. S1B. The peak current increased with increasing accumulation time in the range 20–60 s and then a current plateau was observed as a result of surface saturation. Therefore, 60 s was chosen as the optimal accumulation time for the determination of phenothrin.

3.5. Calibration curve

In order to validate the method for quantitative determination of phenothrin, the variation of the peak current with concentration of phenothrin in phosphate buffer solution (pH 6.5) was studied using square wave voltammetry. The peak current increased linearly with phenothrin concentrations in the range 0.025 μM to 20 μM (Fig. 9). The linear equation is:

$$I(\mu A) = -1.21C(\mu M) + -5.86\ (R^2 = 0.9971) \quad (6)$$

A detection limit of 13.8 nM (S/N = 3) was obtained.

The performance of the GO/PPy/GCE was compared with the report based on hanging mercury drop electrode (HMDE). The result demonstrated that the detection limit of the sensor is better than the detection limit (19 nM) obtained at HMDE [17].

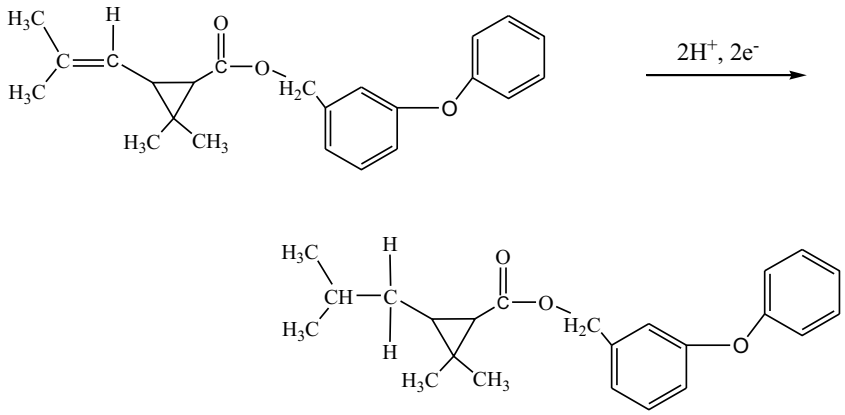

Scheme 1. Mechanism of phenothrin reduction.

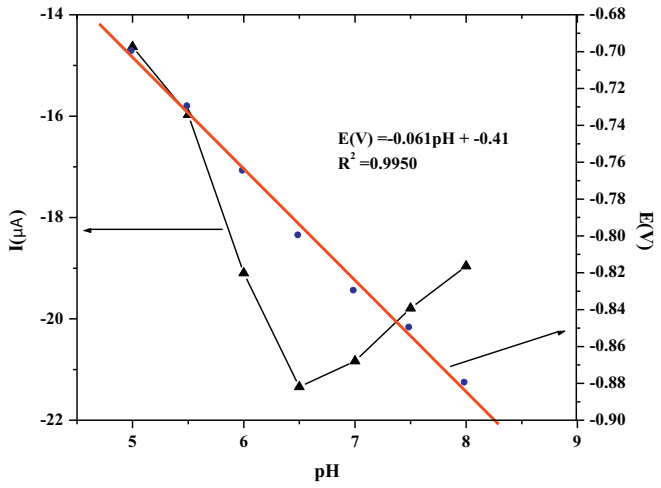

Fig. 8. Plot of peak current and peak potential for 10 μM phenothrin at GO/PPy/GCE in PBS of varying pH.

3.6. Repeatability, reproducibility and stability

The repeatability of the responses of the modified electrode was studied by replicate recordings of the voltammograms for 10 μM phenothrin and a relative standard deviations (RSD) of 4.28% for six consecutive determinations, was obtained. The reproducibility of GO/PPy/GCE electrodes was also evaluated with three different electrodes prepared in the same experimental procedure. The relative standard deviation was found to be 5.1%, demonstrating an excellent detecting reproducibility.

The stability of the sensor was tested by keeping the electrode in 0.1 M phosphate buffer solution (pH 6.5) in a refrigerator at 5 °C. For 10 μM phenothrin solution, the current response of the electrode was found to decrease by 5.6% of its initial value after 7 days of storage. This indicates that the electrode has good stability.

3.7. Interference study

Selectivity of the sensor plays an important role in the determination of analyte in various samples. Investigation was made on species which may affect the signal for phenothrin in fruit samples. The interferents studied were ascorbic acid, citric acid, dichlorvos, phoxim and urea. The results indicated that the presence of 100–fold excess of ascorbic acid, citric acid and urea did not affect the determination of phenothrin (Table 1). Besides, a 10-fold concentration of the two pesticides (dichlorvos, phoxim) showed no interference effect. Thus, these results reveal that GO/PPy/GCE had a good selectivity for phenothrin.

3.8. Applications

To investigate the practical applicability of the developed method, the determination of phenothrin was carried out in commercial juice samples. The samples were prepared according to the procedure described in section 4.4.2. The voltammetric measurements were carried

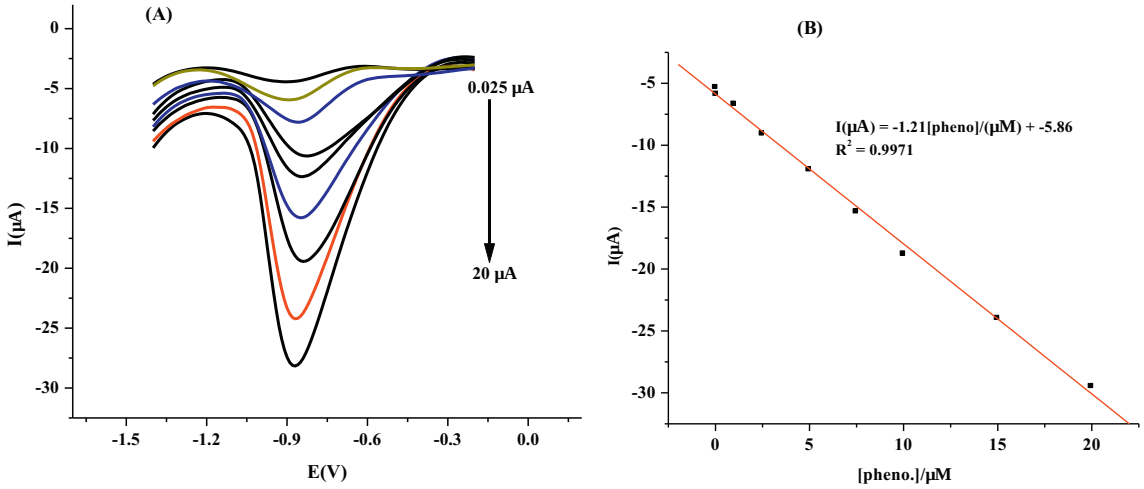

Fig. 9. SWVs of various concentrations of phenothrin (0.025, 0.05, 1.0, 2.5, 5.0, 7.5, 10, 15 and 20 μM) at GO/PPy/GCE (A) and calibration plot of phenothrin (B).

Table 1
Influence of interfering substances on the voltammetric response for 10 μM phenothrin.

Interferences	Concentration ratio ([Interference]/[pheno.]	Signal change (%)
Ascorbic acid	100	−1.5
Citric acid	100	+3.4
Dichlorvos	10	+4.3
Phoxim	10	−5.7
Urea	100	+1.7

Table 2
Recovery study of phenothrin in juice samples (n = 3).

Samples	Added (μM)	Found/μM (± sd)	Recovery (%)
Apple juice	2.5	2.45 (0.08)	98.0
	5.0	4.5 (0.25)	90.0
	10.0	10.3 (0.16)	103.0
Grape juice	2.5	2.56 (0.23)	102.4
	5.0	4.83 (0.42)	96.6
	10.0	10.2 (0.52)	102.0
Orange juice	2.5	2.46 (0.07)	98.4
	5.0	4.74 (0.3)	94.8
	10.0	10.5 (0.46)	105.0

out in apple, grape and orange juices in phosphate buffer solutions. The results did not show any electrochemical response at the peak potential where phenothrin was reduced. This indicates that phenothrine was not available in all the juice samples.

Recovery experiments were performed by spiking the juice (apple, grape and orange) samples with three different concentrations of phenothrin. The results are summarized in Table 2. The recoveries of the spiked samples were in the range 90.0% to 105.0%. It proved that the sensor could be successfully applied for the detection of phenothrin in real samples.

4. Conclusion

A new and sensitive electrochemical sensor for the determination of phenothrin is reported based on graphene oxide-polypyrrole modified glassy carbon electrode. The impedance data confirmed that the decrease in charge transfer resistance (R_{ct}) of the GO/PPy/GCE was significant compared with Go/GCE, PPy/GCE and bare GCE. Besides, cyclic voltammetry results showed that the GO/PPy/GCE exhibited an enhancement in the peak current and shifts of the peak potential towards negative potential. Phenothrin showed an irreversible reaction at GO/PPy/GCE.

The selectivity of GO/PPy/GCE towards phenothrin was investigated in the presence of different interfering species and no significant interference was noted. The stability was evaluated and the signal was found to exhibit a 5.6% decrease for phenothrin reduction. This work demonstrates that the GO/PPy/GCE is a promising electrode material for electrochemical determination of phenothrin.

Supplementary data to this article can be found online at https://doi.org/10.1016/j.sbsr.2018.09.003.

References

[1] C.F. Ramos, D. Satinsky, P. Solich, New method for the determination of carbamate and pyrethroid insecticides in water samples using on-line SPE fused core column chromatography, Talanta 129 (2014) 579–585.
[2] S. Mukdasai, C. Thomas, S. Srijaranai, Two-step microextraction combined with high performance liquid chromatographic analysis of pyrethroids in water and vegetable samples, Talanta 120 (2014) 289–296.
[3] Y. Wang, Y. Sun, Y. Gao, B. Xu, Q. Wu, H. Zhang, D. Song, Determination of five pyrethroids in tea drinks by dispersive solid phase extraction with polyaniline-coated magnetic particles, Talanta 119 (2014) 268–275.
[4] T. Yamada, S. Ueda, K. Yoshioka, S. Kawamura, T. Seki, Y. Okuno, N. Mikami, Lack of estrogenic or (anti-)androgenic effects of d-phenothrin in the uterotrophic and Hershberger assays, Toxicology 186 (2003) 227–239.
[5] Y. Wang, P. Zhang, B. Yang, C. Liu, J. Shu, Kinetic and product study of the heterogeneous reactions of NO3 radicals with suspended resmethrin, phenothrin, and fenvalerate particles, Chemosphere 90 (2013) 848–855.
[6] C. Corcellas, E. Eljarrat, D. Barcelo, First report of pyrethroid bioaccumulation in wild river fish: a case study in Iberian river basins (Spain), Environ. Int. 75 (2015) 110–116.
[7] A. Saillenfait, D. Ndiaye, J. Sabate, Exposure and health effects – an update, Int. J. Hygiene Enviro. Health 218 (2015) 281–292.
[8] D. Wang, D.P. Weston, M.J. Lydy, Method development for the analysis of organophosphate and pyrethroid insecticides at low parts per trillion levels in water, Talanta 78 (2009) 1345–1351.
[9] K. Nagy, G. Racza, T. Matsumotoa, R. Adanya, B. Adam, Evaluation of the genotoxicity of the pyrethroid insecticide phenothrin, Mutat. Res. 770 (2014) 1–5.
[10] H. Yan, J. Du, X. Zhang, G. Yang, K.H. Row, Y. Lv, Ultrasound-assisted dispersive liquid–liquid microextraction coupled with capillary gas chromatography for simultaneous analysis of nine pyrethroids in domestic wastewaters, J. Sep. Sci. 33 (2010) 1829–1835.
[11] I.S. Roman, M.L. Alonso, L. Bartolome, R.M. Alonso, Hollow fibre-based liquid-phase microextraction technique combined with gas chromatography–mass spectrometry for the determination of pyrethroid insecticides in water samples, Talanta 100 (2012) 246–253.
[12] J.H. Borges, S.F. Garcia, A. Cifuentes, M.R. Delgado, Pesticide analysis by capillary electrophoresis, J. Sep. Sci. 27 (2004) 947–963.
[13] F.E. Turrillas, A. Pastor, M. Guardia, Microwave-assisted extraction of pyrethroid insecticides from semi permeable membrane devices (SPMDs) used to indoor air monitoring, Anal. Chim. Acta 560 (2006) 118–127.
[14] J. Dong, X. Wang, F. Qiao, P. Liu, S. Ai, Highly sensitive electrochemical stripping analysis of methyl parathion at MWCNTs–CeO_2–Au nanocomposite modified electrode, Sensors Actuators B 186 (2013) 774–780.
[15] X. Wang, Y. Yang, J. Dong, F. Bei, S. Ai, Lanthanum-functionalized gold nanoparticles for coordination–bonding recognition and colorimetric detection of methyl parathion with high sensitivity, Sensors Actuators B 204 (2014) 119–124.
[16] W. Yazhen, Q. Hongxin, H. Siqian, X. Junhui, A novel methyl parathion electrochemical sensor based on acetylene black–chitosan composite film modified electrode, Sensors Actuators B 147 (2010) 587–592.
[17] T. Thriveni, J. Kumar, J. Lee, N. Sreedhar, Electrochemical determination of phenothrin in agricultural formulations, vegetables, and storage bags of wheat and rice by differential pulse adsorptive stripping voltammetry (DP-AdSV), Food Anal. Methods 2 (2009) 66–72.
[18] B. Paulchamy, G. Arthi, B.D. Lignesh, Simple Approach to Stepwise Synthesis of Graphene Oxide Nanomaterial, J. Nanomed. Nanotechnol. 6 (2015) 1–4.
[19] Z. Qiong, H.Y. Qiu, C.X. Gang, H.D. Hu, L.L. Jiang, Y. Ting, J.L. Li, Structure and photocatalytic properties of TiO_2-Graphene Oxide intercalated composite, Chin. Sci. Bull. 56 (2011) 331–339.
[20] H. Feng, B. Wang, L. Tan, N. Chen, N. Wang, B. Chen, Polypyrrole/hexadecylpyridinium chloride-modified graphite oxide composites: Fabrication, characterization, and application in supercapacitors, J. Power Sources 246 (2014) 621–628.
[21] D. Chen, H. Feng, J. Li, Preparation, functionalization, and electrochemical applications, Chem. Rev. 112 (2012) 6027–6053.
[22] B. Wang, J. Qiu, H. Feng, E. Sakai, Preparation of graphene oxide/polypyrrole/multi-walled carbon nanotube composite and its application in supercapacitors, Electrochim. Acta 151 (2015) 230–239.
[23] V. Singh, D. Joung, L. Zhai, S. Das, S.I. Khondaker, S. Seal, Graphene based materials: past, present and future, Progress in Mater. Sc. 56 (2011) 1178–1271.
[24] T. Qian, C. Yu, X. Zhou, S. Wu, J. Shen, Au nanoparticles decorated polypyrrole/reduced graphene oxide hybrid sheets for ultrasensitive dopamine detection, Sensors Actuators B 193 (2014) 759–763.
[25] W. Lin, H. Chang, R. Wu, Applied novel sensing material graphene/polypyrrole for humidity sensor, Sensors Actuators B 181 (2013) 326–331.
[26] P. A. Basnayaka, M. K. Ram, L. Stefanakos, A. Kumar, Graphene/polypyrrole nanocomposite as electrochemical supercapacitor electrode: electrochemical impedance studies, Graphene 2 (2013) 81–87.
[27] Y. Liu, Y. Zhang, G. Ma, Z. Wang, K. Liu, H. Liu, Ethylene glycol reduced graphene oxide/polypyrrole composite for supercapacitor, Electrochim. Acta 88 (2013) 519–525.
[28] H. Zhou, G. Han, Y. Xiao, Y. Chang, H. Zhai, Facile preparation of polypyrrole/graphene oxide nanocomposites with large areal capacitance using electrochemical codeposition for supercapacitors, J. Power Sources 263 (2014) 259–267.
[29] W. Liu, Y. Fang, P. Xu, Y. Lin, X. Yin, G. Tang, M. He, Two-step electrochemical synthesis of polypyrrole/reduced graphene oxide composites as efficient Pt-free counter electrode for plastic dye-sensitized solar cells, ACS Appl. Mater. Interfaces 6 (2014) 16249–16256.
[30] P.M. Nia, W.P. Meng, F. Lorestani, M.R. Mahmoudian, Y. Alias, Electrodeposition of copper oxide/polypyrrole/reduced grapheneoxide as a nonenzymatic glucose biosensor, Sensors Actuators B 209 (2015) 100–108.
[31] M.F. Hanifah, J. Jaafar, M. Aziz, A.F. Ismail, M.A. Rahman, M.H.D. Othman, Synthesis of Graphene Oxide Nanosheets via Modified Hummers' Method and its Physicochemical Properties, J. Technol. 74 (2015) 195–198.
[32] L. Shahriary, A.A. Athawale, Graphene Oxide Synthesized by using Modified Hummers Approach, International Journal of Renewable Energy and, Environ. Eng. 2 (2014) 1–6.
[33] D.C. Tiwari, P. Atri, R. Sharma, Sensitive detection of ammonia by reduced graphene oxide/ polypyrrole nanocomposites, Syn. Metals 203 (2015) 228–234.

[34] S. Konwer, R. Boruah, S.K. Dolui, Studies on Conducting Polypyrrole/Graphene Oxide Composites as Supercapacitor Electrode, J. Electron. Mater. 40 (2011) 2248–2255.
[35] M. Deng, X. Yang, M. Silke, W. Qiu, M. Xu, G. Borghs, H. Chen, Electrochemical deposition of polypyrrole/graphene oxide composite on microelectrodes towards tuning the electrochemical properties of neural probes, Sens. Actu.B 158 (2011) 176–184.
[36] S. Sahoo, G. Karthikeyan, G.C. Nayak, C.K. Das, Electrochemical characterization of in situ polypyrrole coated grapheme nanocomposites, Synth. Met. 161 (2011) 1713–1719.
[37] W. Lin, H. Chang, R. Wu, Sensors Actuators B 181 (2013) 326–331.
[38] Z. Shi, H. Liu, K. Lee, E. Dy, J. Chlistunoff, M. Blair, P. Zelenay, J. Zhang, Z.S. Liu, J. Phys. Chem. C 115 (2011) 16672–16680.
[39] D.N. Huyen, N.T. Tung, T.D. Vinh, N.D. Thien, Sensors 12 (2012) 7965–7974.
[40] J.V. Thombare, S.K. Shinde, G.M. Lohar, U.M. Chougale, S.S. Dhasade, H.D. Dhaygude, B.P. Relekar, V.J. Fulari, J. Semicond. 35 (2014) 1–4.
[41] G. Lalwani, A.M. Henslee, B. Farshid, L. Lin, F.K. Kasper, Y. Qin, A.G. Mikos, B. Sitharaman, Biomacromolecules 14 (2013) 900–909.
[42] S. Bose, N.H. Kim, T. Kuila, K. Lau, J.H. Lee, Electrochemical performance of a graphene–polypyrrole nanocomposite as a supercapacitor electrode, Nanotechnology 22 (2011) 1–12.
[43] C. Zhao, K. Shu, C. Wang, S. Gambhir, G.G. Wallace, Reduced graphene oxide and polypyrrole/reduced graphene oxide composite coated stretchable fabric electrodes for supercapacitor application, Electrochim. Acta 172 (2015) 12–19.
[44] X. Zhang, D.C. Zhang, Y. Chen, X.Z. Sun, Y.W. Ma, Electrochemical reduction of graphene oxide films: Preparation, characterization and their electrochemical properties, Chin. Sci. Bull. 57 (2012) 3045–3050.
[45] C. Fu, G. Zhao, H. Zhang, S. Li, Evaluation and characterization of reduced graphene oxide nanosheets as anode materials for lithium-ion batteries, Int. J. Electrochem. Sci. 8 (2013) 6269–6280.
[46] E. Laviron, General expression of the linear potential sweep voltammogram in the case of diffusionless electrochemical systems, J. Electroanal. Chem. 101 (1979) 19–28.